

Highly catalytic performance of novel Ni-Cu containing SBA-15 materials in the hydrodeoxygenation of guaiacol

Tuan A. Vu^{1,*}, Giang H. Le¹, Giang T. T. Pham², Hoa T.K. Tran¹, Phuong T. Dang¹, Manh B. Nguyen¹, Loi D. Vu¹, Gun D. Lee³

¹Institute of Chemistry-VAST, 18 Hoang Quoc Viet street, CauGiay District, Hanoi City, Vietnam

²Hanoi University of Industry, BacTuLiemDistric, Hanoi City, Vietnam

³College of Engineering, Pukyong National University, Yongdang Campus, Busan, South Korea

*corresponding author e-mail address: vuanhtuan.vast@gmail.com

ABSTRACT

Bimetallic Ni-Cu containing SBA-15 materials were successfully synthesized by direct and impregnation methods. The samples were characterized by XRD, FTIR, TEM, EDX, BET, H₂-TPR and XPS. From TEM images, it showed that the Ni-Cu-SBA-15 by direct synthesis had the very small size of Ni and Cu particles (1-2 nm), existed as isolated atoms while the Ni-Cu/SBA-15 by impregnation method had the particle size of 50-100 nm., but metal particles existed as aggregated form. In the hydrodeoxygenation(HDO)of guaiacol over two catalysts it revealedthat theNi-Cu-SBA-15 by direct synthesis exhibited much higher catalytic performance as compared to that of Ni-Cu/SBA-15 by impregnation method, especially HDO efficiency of this catalyst was two times higher than that of Ni-Cu/SBA15.From this result, it clearly demonstrated the effectiveness of isolated atoms as highly active sites in catalytic conversion of organic compounds.

Keywords: Ni-Cu bimetallic catalysts, SBA-15 nanopore-size materials, direct methods, wet impregnation.

1. INTRODUCTION

The depletion of fossil fuels and environmental concerns have prompted the research to look for alternative sources of energy and chemicals. Lignocellulosic biomass is one of the important sources of renewable feedstock and by fast pyrolysis technology, bio-oil can be produced at the industrial scale [1]. However, this bio-oil can not be directly used as fuel due to high oxygen content, low heating value, high viscosity, incomplete volatility and thermal instability. In order to upgrade the bio-oil, hydrodeoxygenation process of bio-oil is the most promising route for producing liquid transportation fuel.

Currently, catalysts for the hydrogenation of organic compounds, hydrodeoxygenation of oxygen-containing organic compounds, especially for oil and bio-oil upgrading have attracted great attention in the field of catalysis. The catalysts for this process are usually noble metals (Pt, Pd, Ru, Rh,...) on the SiO₂-Al₂O₃, CeO₂-ZnO₂, SiO₂, MgO, ZrO₂ and activated carbon support [1]. The noble metal catalysts have high catalytic activity, but they are expensive and fast poisoned leading to their limited application potential. Currently, studies focused on the non-noble metal catalysts with low cost. Nickel based catalyst is one of best alternates to be used as active metal in hydrogenation reaction of organic compounds. Ni- based catalysts exhibit quite high activity for hydrogenation, hydro deoxygenation [2, 3]. Nickel is often associated with some other metals such as Cu, Mo, Fe, which can

decrease the reduction temperature of nickel oxide and the coke formation rate on surface of catalysts [3, 4]. In preparation of nickel-based catalyst, oxides like SiO₂, ZrO₂, CeO₂-ZnO, MgO are widely used as supports. However, most these oxides have low surface area, limiting the dispersion of nickel particles on the surface. To increase the dispersion, nickel is deposited on the mesoporous materials which have very high surface area such as MCM41, MCM48, SBA15. Thus, in the most studies reported in the literature showed that the catalytic activity in the bio-oil hydro deoxygenation was improved by using mesoporous materials as supports [5]. Nickel based catalysts have been synthesized by methods including precipitation, impregnation and ion exchange. Recently, investigations on nickel supported MCM-41, MCM-48, SBA-15 mesoporous materials have been reported [6 -10]. In these papers, they revealed that Ni supported on mesoporous materials exhibited relative high catalytic activity and ability to replace the traditional catalysts containing metals Pt, Ru. However, bimetallic supported on mesoporous materials like Ni with Cu, Co, Mn, etc were still rarely investigated.

In this paper, we report the synthesis bimetallic Ni - Cu containing SBA-15 using impregnation and direct synthesis (incorporating Ni, Cu into SBA-15 structure) method. Catalytic performance of these samples were evaluated and discussed.

2. EXPERIMENTAL SECTION

2.1. Materials synthesis. Synthesis of SBA-15 material: 1g of surfactant P123 was dissolved in 60ml of HCl solution (2M concentration) and stirred for few hours until to get a clear

solution. Sodium silicate solution containing 2g of SiO₂ equivalent was added drop-wise into surfactant solution under vigorous stirring for 2 hours at room temperature and then the mixture was

further stirred for 24 hours at 45°C. Finally, the obtained mixture was poured into Teflon-lined autoclave and hydrothermally treated at 100°C for 24 hours. The solid product was washed, dried at 80°C overnight, and calcined in an oven at 550°C for 6 hours to remove surfactant.

Synthesis of Ni-Cu-SBA-15 (direct synthesis): 1g of surfactant P123 was dissolved in 60ml of HCl solution (2M concentration) and stirred for few hours until to get a clearly surfactant solution. Sodium silicate solution containing 2g of SiO₂ equivalent was added drop-wise into surfactant solution. To this surfactant solution, 1.337g Ni(NO)₂.6H₂O and 0.375 g Cu(NO)₂.3H₂O were added to the surfactant solution and stirred for an hour until the solution become clear. Then the next steps were similar to those of SBA-15 synthesis. The obtained sample was denoted Ni-Cu-SBA-15(di).

Ni-Cu/SBA-15 (post synthesis) was prepared by the impregnation of Ni and Cu salts on SBA-15 material. 1.377g Ni(NO)₂.6H₂O and 0.375g Cu(NO)₂.3H₂O were dissolved in 10 ml of distilled water. Then 2g SBA-15 (calcined form) were added into this salt solution. The mixture was stirred for 2 hours, dried at 80°C for 10 hours and calcined at 500°C for 3 hours. The resulting sample was denoted Ni-Cu/SBA-15(im).

2.2. Characterization of catalyst. X-ray diffraction (XRD) patterns of the samples determined by X-ray diffraction technique on a Bruker D8 ADVANCE in the 2θ angle in the range of 0.5–100 and 10-900. Adsorption-desorption experiments using N₂

(BET) were carried out at 77K on a Micromeritic Tristar 3000 equipment. The N₂ isotherms were used to determine the specific surface areas and pore volumes, diameters of the samples using the BET equation and BJH theory. Transmission electron microscopy (TEM) images of materials were obtained on a JEM 1010. Energy diffraction X-ray (EDX) pattern measured on a Station Analysis JED-2300 to determine elemental concentrations. UV-vis diffuse reflectance spectra of the samples were obtained on a Lambda 35- PerkinElmer spectrometer with BaSO₄ used as standard measurements. The XPS spectra was carried out on thermo VG scientific (UK), multilab 2000. H₂-TPR was carried out in a AutoChem 2920 of Micromeritics (USA).

2.4. Catalytic activity test. The HDO reaction of guaiacol was carried out in a 300ml stainless steel batch autoclave equipped with a magnetic stirring. The reaction system was heated with an automatic temperature control device and magnetic stirring speed was kept at 700 rpm. Before the reaction, the Ni based catalysts were reduced in the reactor by in a flow of the mixture of 35% H₂ and 65% Ar (100ml/min) at 400°C for 4 hours. For each run, 2g catalyst and 30ml of guaiacol were used. After displacing air in the autoclave the reactor was pressurized with the mixture of 35% H₂ and 65% Ar to 50bar and sealed. The reaction temperature was heated to 320°C and the time reaction was 3h. The liquid products were identified by GC-MS with column RTX Wax (30m x 0.25mm id x 0.25m df).

3. RESULTS SECTION

3.1. Catalyst characterization

3.1.1. X-ray diffraction (XRD). Figure 1 showed the low-angle X-ray diffraction patterns of SBA-15, Ni-Cu-SBA-15(di) and Ni-Cu/SBA-15(im) samples. As observed in fig.1, one peak with strong intensity at the 2θ of ~1.02° and two peaks with weak intensity at 2θ of ~1.6° and ~1.8°, correspond to the diffraction of (100), (110) and (200) reflection, respectively. These are characteristic for the structure of 2D hexagonal *p6mm* symmetry of mesoporous SBA-15 structure [7, 11].

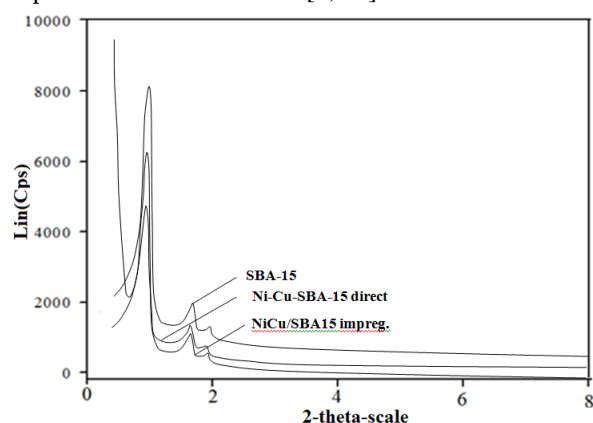


Figure 1. The low angle XRD patterns and of SBA-15, Ni-Cu-SBA-15(di) and Ni-Cu/SBA-15(im).

In the wide angle XRD patterns of the Ni-Cu-SBA-15(di) (not shown here), no diffraction lines of Ni and Cu phase appeared. This may be due to the low metal contents in the Ni-Cu-SBA-15 sample which cannot be detected by XRD. In the case of

Ni-Cu/SBA-15(im) the diffraction peaks at 2θ of 37.36, 43.32 and 64.84° appeared which are characteristic for the cubic crystalline of NiO, and two peaks at 2θ of 35.4 and 38.7° attributed for copper crystalline phase. This result can be explained by the fact that high Ni and Cu content in the sample (see EDX result below) which enabled to be detected by XRD.

3.1.2. N₂ adsorption and desorption (BET). The N₂ adsorption and desorption data for Ni-Cu-SBA-15(di) and Ni-Cu/SBA-15(im) were summarized in table 1.

Table 1. The structural parameters of the SBA-15 and Ni - Cu - SBA-15 and Ni-Cu/SBA-15 materials.

Sample	S _{BET} (m ² /g)	S _{meso} (m ² /g)	S _{micro} (m ² /g)	V _{pore} (cm ³ /g)	D _{BJH} (nm)
SBA-15	622	429	193	0,878	7,1
Ni-Cu-SBA-15(di)	583	466	117	1,117	9,0
Ni-Cu/SBA-15(im)	470	365	104	0,762	5.6

S_{meso}: surface area of the mesopore, S_{micro}: surface area of the micropore, D_{BJH}: pore diameter, V_{pore}: pore volume

As seen in table 1, Ni-Cu/SBA-15 sample has lower surface area, pore volume and pore diameter, as compared to those of SBA-15. This can be explained by the fact that the deposition of Ni and Cu nano particles on Sba-15 surface caused the decrease of N₂ adsorption sites and consequently decreased the surface area. Location of Ni and Cu nano particles within the pore system also

caused the decrease of pore volume and pore diameter. By contrast, Ni-Cu-SBA-15 has larger volume pore and pore diameter as compared to those of Ni-Cu/SBA-15. This may be due to the very low deposition Ni, Cu amount which well dispersed and inserted into pore walls of SBA-15 and new meso-pores formed by space created between Ni,Cu small particles.

3.1.3. Transmission electron microscopy (TEM). TEM images show two dimensional hexagonal structures of all samples. No individual metal oxide particles were observed in the TEM image of Ni-Cu-SBA-15 direct synthesis sample (Fig.2a), indicating high dispersion of the metal in the mesoporous material. The TEM of Ni-Cu/SBA-15(im) shows the presence of clear dark metal oxide crystallites with large size of about 50-100nm at the external surface of SBA-15 material (Fig.2c), which can block the pores partially.

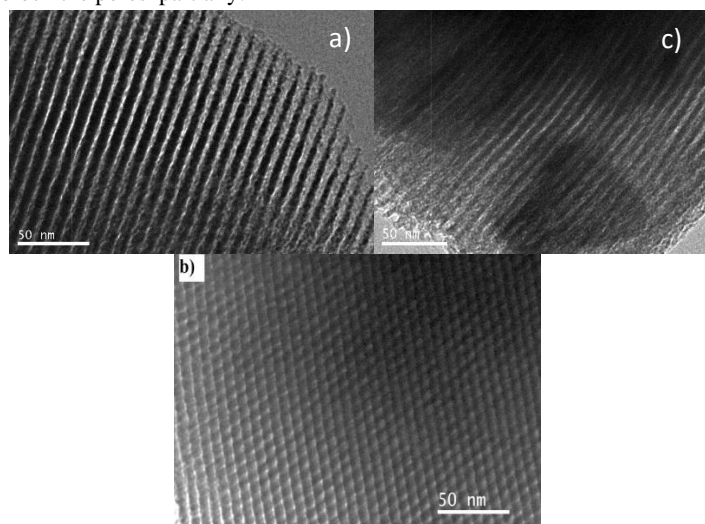


Figure 2. TEM images of SBA-15 silica (b), Ni-Cu-SBA-15(di) (a), Ni-Cu/SBA-15(im) (c).

3.1.4. Energy X-ray diffraction (EDX). The results chemical compositions of Ni, Cu, Si and O elements for Ni-Cu/SBA-15 and Ni-Cu-SBA-15 samples determined by EDX are given in the table 2.

Table 2. Element contents of O, Si, Ni, Cu for Ni-Cu/SBA-15 and Ni-Cu-SBA-15.

Sample	Element content (wt.%)			
	O	Si	Ni	Cu
Ni-Cu-SBA-15(di)	62.85	36.21	0.48	0.46
Ni-Cu/SBA-15(im)	48.31	33.08	13.75	4.86

As observed in table 2, the Ni and Cu amounts 0.48 wt.% and 0.46 wt.% of the Ni-Cu-SBA-15 (di) sample were are much lower in comparison to those introduced in the gel (14 and 5% respectively). This may be due to the fact that synthesis was performed in strong acidic condition (pH<1), Ni and Cu salts dissolved in the solution, only very small amount of Ni, Cu could be inserted into SBA-15 frameworks. Ni and Cu content in the case of Ni-Cu/SBA-15 (im) was not differentiated between synthesis gel and soil products and ca.20 times higher than that of Ni-Cu-SBA15.

3.1.5. UV-vis diffuse reflectance spectroscopy. The UV-vis spectra of samples were presented in Figure 3. In general, the intensity of adsorption band increases with the increase of Ni and Cu content in the samples, while the silica SBA-15 almost has no this adsorption band. The band appears at 220nm, corresponding to isolated metal sites (metal ions incorporated into silica matrix or ion-exchanged with Si-OH groups). The band at 320nm observed on the Ni-Cu-

SBA-15(di) and Ni-Cu/SBA-15(im) corresponded to the presence of very low-polymeric Me-O-Me species and the band at 450 nm attributed to the high polymeric Me-O-Me ones[12, 13].

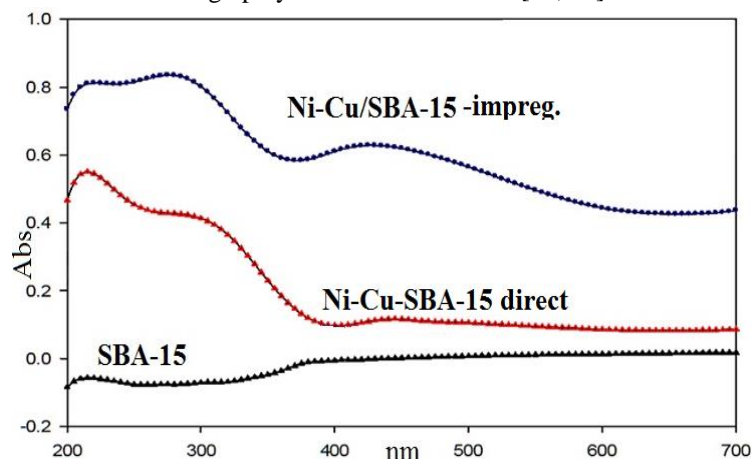


Figure 3. UV-vis spectra of SBA-15 silica, and Ni-Cu supported SBA-15 samples.

3.1.6. H₂-TPR of the catalysts. The H₂-TPR profiles of Ni-Cu-SBA-15(di) and Ni-Cu/SBA-15(im) samples were given in Fig.4. In the case of Ni-Cu/SBA-15(im), there are two main peaks, the first peak centered at 210°C, and other one centered at 250°C. These peaks can be attributed to reduction peaks of CuO and NiO on SBA-15 support. According to [1, 2] the reduction peak of well-crystallized NiO and CuO are centered at 400°C, and at 230-300°C, respectively.

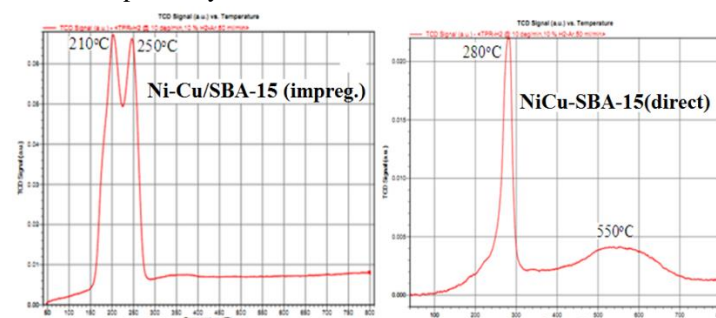


Figure 4. H₂-TPR patterns of Ni-Cu/SBA-15(im) and Ni-Cu-SBA-15(di) samples.

For the Ni-Cu-SBA-15(di) prepared by direct incorporation method, the H₂-TPR profile also had two main peaks centered at 280°C and the at 550°C, respectively. The high temperature required for reduction may be due to Ni and Cu in this material incorporated into the SBA-15 framework by the formation of the Si-O-Ni bonds and Si-O-Cu and/or the interaction between Ni,Cu with Si of SBA15[14].

3.1.7. XPS study. Figure 5 showed the XPS spectra of Cu2p and Ni2p core level regions for Ni-Cu/SBA-15 (di) and Ni-Cu-SBA-15(im). In the spectrum of Ni-Cu-SBA-15 (im), Ni2p levels appeared the main peak at 858 eV and three peaks at 865 eV; 880 eV and 858 eV while Cu2p appeared two peaks at 935 and 855 eV. These peaks reflected the different states of Ni and Cu, similar to those reported in the literature [3]. In the case of Ni-Cu-SBA-15 (di) the main peaks for Ni2p levels appeared at the same binding energy but much lower intensities as observed on Ni-Cu/SAB-15 (im). However, Cu2p levels did not show the peaks. This can may be due to the very low content of Cu and/or the strong interaction between Cu and Si-OH groups in the SBA-15 matrix.

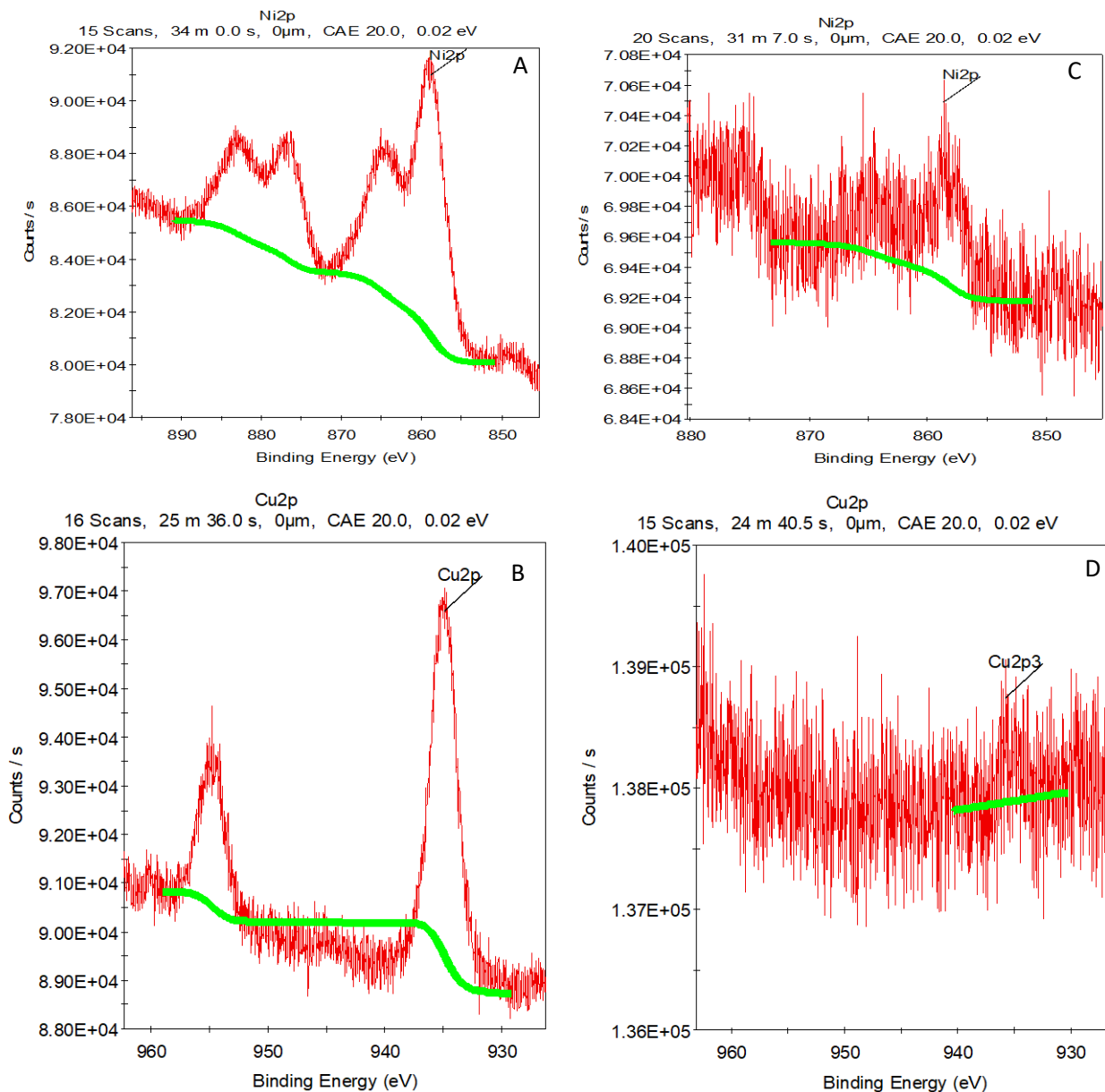


Figure 5. The Ni2p and Cu2p core level spectra of Ni-Cu/SBA-15(im) (a, b), and Ni-Cu-SBA-15(di) samples (c, d).

3.2. Hydrodeoxygenation of guaiacol. The hydrodeoxygenation of guaiacol over Ni-Cu/SBA-15(im) and Ni-Cu-SBA-15(di) catalysts was carried at 320°C, reaction time of 3 hours, and hydrogen pressure of 17.5 bar. The guaiacol conversion and selectivity towards the main products were presented in table 3.

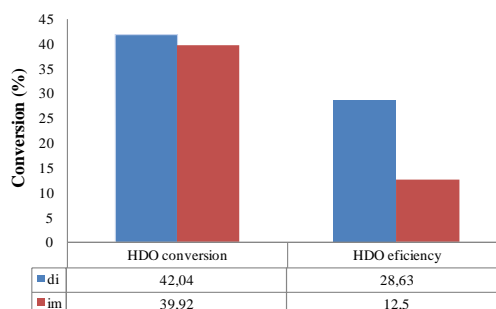
As observed in table 3, Ni-Cu-SBA-15 (di) had higher conversion as compared to that of Ni-Cu/SBA-15 (im). Note that Ni-Cu-SBA-15 (di) with the Ni and Cu content (ca. 0.9%wt) is much lower (ca.20 times) than that of Ni-Cu/SBA-15 (im). This clearly indicated the much higher catalytic effectiveness of Ni, Cu sites in Ni-Cu-SBA-15 (di) sample. This may be due to the very small size of nano particles (at atomic scale) were created and well dispersed on SBA-15 surface as observed by HR-TEM images. Moreover, hydro-deoxygenation (HDO) efficiency of Ni-Cu-SBA-15 (di) sample is also higher (two times) as compared to that of Ni-Cu/SBA-15 (im), showing much higher catalytic selectivity of this sample. This can be explained that Ni, Cu atoms formed on the large surface of SBA-15 structure promoted the reduction of phenol to benzene and cyclohexane, consequently HDO selectivity was enhanced [15, 16]. Moreover, in comparison with 1%Pt/SBA-

15 and 1%Ru/SBA15 tested under the same reaction condition had the conversion of 38-43%, similar to that of Ni-Cu-SBA15(di) .

Table 3. Production distribution and conversion of guaiacol over catalysts.

Catalyst	Ni-Cu/SBA-15(im)	Ni-Cu-SBA-15(di)
Conversion (%)	39.92	42.04
HDO efficiency	12.5	28.6
Production distribution (%)		
Phenol	60.57	33.85
Methoxybenzen	36.93	37.52
Benzen	10.39	21.12
Cyclohexan	2.11	7.51

Figure 6. HDO: The Hydrodeoxygenation products include benzene and cyclohexan



4. CONCLUSIONS

Bimetallic Ni-Cu containing SBA-15 materials were successfully synthesized by impregnation and incorporation methods. From characterization results, it revealed the formation of nano Ni and Cu particles on SBA-15 surface. However, Ni-Cu-SBA-15 prepared by direct synthesis (incorporation of Ni, Cu into SBA-15 structure) showed much lower Ni, Cu particles size of 1-2

nm (atomic scale) and very high dispersion degree on SBA-15 surface. In hydrodeoxygenation of guaiacol, both Ni-Cu containing SBA-15 exhibited high catalytic activity but Ni-Cu-SBA-15 prepared by direct synthesis showed much higher catalytic effectiveness as compared to that of Ni-Cu/SBA-15 synthesized by impregnation method.

5. REFERENCES

- [1]. Choudhary T.V., Phillips C.B., Renewable fuels via catalytic hydrodeoxygenation, *Applied Catalysis A: General*, 397, 1-12, **2011**.
- [2]. Xinghua Z., Tiejun W., Longlong M., Qi Z., Ting J., Hydro-treatment of bio-oil over Ni-based catalyst, *Bioresource Technology*, 127, 306-311, **2013**.
- [3]. Bykova M.V., Yu D., Ermakov V.V., Kaichev O.A., Bulavchenko A.A., Saraev M., Yu Lebedev, Yakovlev V.A., Ni-based sol-gel catalysts as promising systems for crude bio-oil upgrading: Guaiacol hydrodeoxygenation study, *Applied Catalysis B: Environmental*, 113(114), 296-307, **2012**.
- [4]. Ardiyanti A.R., Khromova S.A., Venderbosch R.H., Yakovlev V.A., Heeres H.J., Catalytic hydro-treatment of fast-pyrolysis oil using non-sulfided bimetallic Ni-Cu catalysts on a δ -Al₂O₃ support, *Applied Catalysis B: Environmental*, 117(118), 105-117, **2012**.
- [5]. Yuxin W., Jinhua W., Shengnian W., Hydrodeoxygenation of bio-oil over Pt-based supported catalysts: importance of mesopores and acidity of the support to compounds with different oxygen contents, *RSC Adv.*, 3, 12635-12640, **2013**.
- [6]. Heejin L., Hannah K., Mi Jin Y., Chang H.K., Jong-Ki J., Jungho J., Sung H.P., Sang-Chul J., Young-Kwon P., Catalytic Hydrodeoxygenation of Bio-oil Model Compounds over Pt/HY Catalyst, *Sci Rep*; 6, 28765, **2016**.
- [7]. Rafael H.A., Rufino N., Carmen L. Peza-Ledesma, Javier Lara-Romero, Gabriel Alonso-Núñez, Barbara P., Eric M. Rivera-Muñoz, SBA-15 Mesoporous Silica as Catalytic Support for Hydrodesulfurization Catalysts—Review, *Materials*, 6, 4139-4167, **2013**.
- [8]. Songbai Q., Ying X., Yujing W., Longlong M., Tiejun W., Efficient Hydrogenolysis of Guaiacol over Highly Dispersed Ni/MCM-41 Catalyst Combined with HZSM-5, *Catalysts*, 6, 134, **2016**.
- [9]. Infantes-Molina A., Gralberg E., Cecilia J.A., Elisabetta F., Rodríguez-Castellón E., Nickel and cobalt phosphides as effective catalysts for oxygen removal of dibenzofuran: role of contact time, hydrogen pressure and hydrogen/feed molar ratio, *Catal. Sci. Technol.*, 5, 3403-3415, **2015**.
- [10]. Sharafadeen G., Tammar H.A., Lee H.V., Abdulazeez Y.A., Putla S., Suresh K. Bhargava, Sharifah Bee A.H., Promising Ni/Al-SBA-15 catalysts for hydrodeoxygenation of dibenzofuran into fuel grade hydrocarbons: synergistic effect of Ni and Al-SBA-15 support, *RSC Adv.*, 6, 25992-26002, **2016**.
- [11]. Ajayan V., Toshiyuki M., Katsuhiko A., New families of mesoporous materials, *Science and technology of Advanced materials*, 7, 753-771, **2006**.
- [12]. Shah P., Ramaswamy A.V., Lazar K., Veda R., Direct hydrothermal synthesis of mesoporous Sn-SBA-15 materials under weak acidic conditions, *Microporous and Mesoporous materials*, 100, 210-226, **2007**.
- [13]. Timofeeva M.N., Jung S.H., Hwang Y.K., Kim D.K., Panchenko V.N., Melgunov M.S., Yu. A.C., Chang J.S., Ce-silica mesoporous SBA-15-type materials for oxidative catalysis: Synthesis, characterization, and catalytic application, *Applied Catalysis A: General*, 317, 1-10, **2007**.
- [14]. Gerardo V., Hebert M., Eumir H., Samuel A., Viola B., Pedro P.-A., One-pot preparation and characterization of bifunctional Ni-containing ZSM-5, *Applied Catalysis A: General*, 452, 75-87, **2013**.
- [15]. Tyrone Ghampson I., Catherine Sepulveda, Rafael Garcia, Garcia Fierro J.I., Nestor Escalona, William J. Desisto., Comparison of alumina- and SBA-15-supported molybdenum nitride catalysts for hydrodeoxygenation of guaiacol, *Applied Catalysts A: General*, 435(436), 51-60, **2012**.
- [16]. Bui V.N., Tousling G., Laurenti D., Microdots C., Geanter C., Co-processing of pyrolysis bio oils and gas oil for new generation of bio-fuels: Hydrodeoxygenation of guaiacol and SRGO mixed feed, *Catalysis Today*, 143, 172-178, **2009**.

6. ACKNOWLEDGEMENTS

The authors thank the Vietnam Academy of Science and Technology-VAST for financial support project (VAST.2016-VuAnhTuan).

© 2018 by the authors. This article is an open access article distributed under the terms and conditions of the Creative Commons Attribution license (<http://creativecommons.org/licenses/by/4.0/>).